AAPS PharmSciTech, Vol. 14, No. 1, March 2013 (© 2012)
DOI: 10.1208/s12249-012-9906-0

Research Article

Investigation on Side-Spray Fluidized Bed Granulation with Swirling Airflow

Poh Mun Wong,[1] Lai Wah Chan,[1] and Paul Wan Sia Heng[1,2]

Received 13 October 2012; accepted 29 November 2012; published online 21 December 2012

Abstract. Top-spray fluidized bed granulation with axial fluidization airflow from the bottom of the granulator is well-established in the pharmaceutical industry. The application of swirling airflow for fluidized bed granulation was more recently introduced. This study examined the effects of various process parameters on the granules produced by side-spray fluidized bed with swirling airflow using the central composite and Box–Behnken design of experiment. Influence of the amount of binder solution, spray rate, and distance between spray nozzle and powder bed were initially studied to establish operationally viable values for these parameters. This was followed by an in-depth investigation on the effects of inlet airflow rate, atomizing air pressure and distance between spray nozzle and powder bed on granule properties. It was found that the amount of binder solution had a positive correlation with granule size and percentage of lumps but a negative correlation with size distribution and Hausner ratio of the granules. Binder solution spray rate was also found to affect the granules size. High drug content uniformity was observed in all the batches of granules produced. Both inlet airflow rate and atomizing air pressure were found to correlate negatively with granule size and percentage of lumps but correlate positively with the size distribution of the granule produced. Percentage of fines was found to be significantly affected by inlet airflow rate. Distance between spray nozzle and powder bed generally affected the percentage of lumps.

KEY WORDS: Box–Behnken design; central composite design; fluidized bed granulation; swirling airflow.

INTRODUCTION

Since its introduction by Wurster, the fluidized bed processor has been widely used in the pharmaceutical industry for mixing, granulation, drying, and coating. Many studies had been carried out to investigate the various aspects of fluidized bed granulation, with the majority focusing on the top-spray fluidized bed granulation (1–7). Various innovative modifications of the fluidized bed granulator had resulted in different designs that produced granules with different properties. Depending on the position of the spray nozzle in the equipment, fluidized bed granulators could be classified as top spray, bottom spray, or tangential spray (Fig. 1a–c). The advantages and disadvantages of these fluidized bed granulators are briefly highlighted in Table I.

Due to the rising cost of energy and the need to be efficient, the long processing time of top spray and bottom spray fluidized bed granulators is a pertinent area for improvement. The long processing time is mainly due to the relatively lower liquid spray rate employed. Spray rate ranging from about 4.5–12 g/min was adopted in a study using top-spray fluidized bed granulator with a 2.5 kg batch (8). In another study, spray rate ranging from about 10–17 g/min was used for a 1 kg batch in a bottom spray granulator (9). Very high liquid spray rate is not suitable for these granulators as it would result in excessive wetting of the powder bed, leading to a possible "wet quenching", where large regions of the bed might defluidize and agglomerate as large wet clumps (10). A fluidized bed system that can accommodate a high liquid spray rate is preferred in order to shorten the processing time and improve production efficiency without adversely affecting product quality. This would only be possible if the evaporative efficiencies in the fluidized bed system can be improved. In addition, it was observed that the homogeneous rope-like movement of the powder bed in the tangential spray fluidized bed granulator allowed for considerably higher binder solution spray rate as well as possibly better agglomerated product quality. This led to the development of the FlexStream™ fluidized bed process, where the efficiencies of centrifugal processing and high evaporative rate are combined.

The FlexStream™ fluidized bed processor can be employed for granulation, drying, and pellet coating. It consists of a dual-fluid spray nozzle inserted from the side of product chamber to deliver the granulation or coating liquid (Fig. 1d). Surrounding this nozzle is a low pressure air used to create a particle-free zone around the spray nozzle to prevent local overwetting. This low pressure air is supplied from the plenum *via* a tube that links the product chamber directly with the inlet air plenum. Since air is taken from the inlet air plenum, it is conditioned in the same way as the main fluidization air. Coupled with a patented nonsifting gill plate to distribute the air from the bottom of the product chamber, a swirling flow pattern is generated within the chamber. Swirling

[1] GEA-NUS Pharmaceutical Processing Research Laboratory, Department of Pharmacy, National University of Singapore, 18 Science Drive 4, Singapore 117543, Singapore.
[2] To whom correspondence should be addressed. (e-mail: phapaulh@nus.edu.sg)

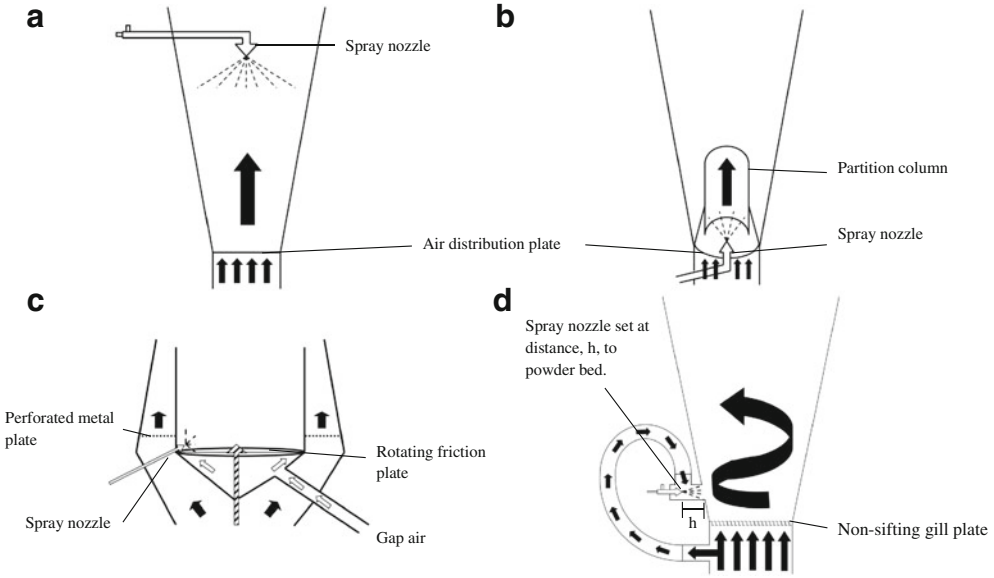

Fig. 1. Schematic diagrams of **a** top spray, **b** bottom spray, **c** tangential spray, and **d** FlexStream™ fluidized bed granulators. *Dark arrows* in the diagrams indicate airflow pattern

flow pattern of air had been extensively studied as being capable of higher airflow rate and improved heat transfer (11–13). The swirling flow pattern thus allows higher liquid spray rate with the improved drying efficiency, enabling a shorter granulation process time.

This study aimed to achieve a good understanding of the FlexStream™ fluidized bed process using a design of experiment (DOE) approach. A central composite design was adopted for optimization of the process. The amount of binder liquid (14,15) and binder spray rate (2,16,17) are known to affect granule growth. Furthermore, Davies *et al.* (16) had previously shown that in top-spray fluidized bed granulation, the closer the nozzle was positioned to the fluidizing powder bed, the better was the ability to wet and penetrate the fluidized solids, resulting in larger granules. Hence, three variables, namely amount of binder solution, binder solution spray rate, and distance between nozzle and powder bed were selected for investigation. After optimization, the selected variables were used for a second DOE study to further examine the effects of airflow rate, atomizing air pressure, and distance between nozzle and powder bed. The findings of the above investigations would establish the capability of the FlexStream™ fluidized bed process for high-speed granulation without compromising on the quality of the granules produced.

MATERIAL AND METHODS

Material

Commercially available α-lactose monohydrate (GranuLac 200, Meggle Excipients and Technology, Germany) was used as feed powder for fluidized bed granulation. Two grades of polyvinylpyrollidone, Povidone K25 and Povidone K90 (PVP-K25 and PVP-K90; ISP Technologies, USA), were used for the preparation of binder solution. Chlorpheniramine maleate (BP grade, China) was used as a model drug.

Table I. Advantages and Disadvantages of Various Types of Fluidized Bed Granulators

Fluidized bed granulator	Advantages	Disadvantages
Top spray	More porous granules (18)	Granules are irregular in shape (18)
	"One-pot" system for contained production (19)	More spray drying of binder solution
Bottom spray	Smaller granules (20)	Denser granules (20,21)
	Spherical granules with better flow (21)	Slower granule growth (20)
	Smoother surface granules (22)	Higher risk of overwetting
	Less spray drying of binder solution (23)	Need reasonably well flowing feed powders
	Robust process at low spray rate (21).	
Tangential spray	Supports higher spray rate (24,25)	Denser granules (25,26)
	Less dependent on flow properties of powder feed (26)	Material loss due to adhesion to friction plate (26)
	Powder elutriation only at higher airflow (24)	Scale-up designs are expensive and impractical
	Granule growth is relatively uniform (25)	Risk of bed overwetting is high
	Granules have good flow properties (25,26)	
	Granules have low friability (25)	
	Homogeneous drug distribution (26)	

Methods

Granulation Process

The granulation process was conducted with a FlexStream™module which was mounted on an air handling system (MP-1 Multi-processor, GEA Aeromatic-Fielder, UK). For each run, 1.9 kg of lactose was granulated in a conical acrylic product chamber with binder solution containing PVP-K25 (15%, *w*/*w*), PVP-K90 (5%, *w*/*w*), and CFM (6.66%, *w*/*w*). The operating parameters and variables employed are shown in Tables II and III.

At the end of each granulation run, the content of the chamber was carefully collected and weighed. The yield was then calculated by:

$$Yield = \frac{W_f}{W_i + W_s} \times 100\% \quad (1)$$

where W_f is the weight of collected product, W_i is the load used for granulation, and W_s is the dry weight of solids added *via* the spray solution.

Design of Experiment

Part 1

A central composite design was employed to study the influence of the following parameters: (a) amount of binder solution delivered, X_1; (b) binder solution spray rate, X_2; and (c) distance between spray nozzle and powder bed, X_3, contributing to the design variables. The settings of the design are shown in Table IIIa. The α value in central composite design dictates the position of the axial point. By choosing a default α value, the central composite design ensures that the design is rotatable. Rotatable designs allow constant prediction variation at all points that are equidistant from the design center, therefore improving the quality of prediction. Hence, this is a desirable condition for the design. However, it was difficult to adopt a default value due to the need for setting some process parameters. Hence, the default α value of 1.633 was rounded up to 2, for ease of setting parameter values for the experiments.

Table II. Operating Parameters Employed in FlexStream™ Granulation

Variables	Operating parameters	
	Part 1	Part 2
Inlet airflow rate (m^3/h)[a]	80~140	As in DOE
Atomizing air pressure (bar)	2.5	As in DOE
Inlet air temperature (°C)	60	60
Drying time (min)	10	10
Drying airflow rate (m^3/h)[a]	140~80	100
Nozzle tip diameter (mm)	0.8	0.8
Nozzle tip protruded level (mm)	1.2	1.2
Amount of binder solution delivered (g)	As in DOE	415
Binder solution spray rate (g/min)	As in DOE	60
Distance between spray nozzle and powder bed (mm)	As in DOE	As in DOE

[a] Variable, dependent on the amount of binder solution and binder solution spray rate employed, sufficient for fluidization

Table III. Settings of Statistical Designs Used

Design variables	Settings	
	Low level	High level
(a) Part 1: central composite design		
X_1	350	450
X_2	55	65
X_3	12	16
α	2	
(b) Part 2: Box–Behnken design		
X_4[a]	80	120
X_5	1.5	3.5
X_6	10	18

X_1 Amount of binder solution delivered (grams), X_2 binder solution spray rate (grams per minute), X_3 distance between spray nozzle and powder bed (millimeters), X_4 inlet airflow rate (cubic meters per hour); X_5 atomizing air pressure (bar), and X_6 distance between spray nozzle and powder bed (millimeters)

[a] Inlet airflow rate increased by 10 m^3/h after 200 g binder solution was delivered and another 10 m^3/h after 350 g binder solution was delivered

Based on the settings, a total of 20 experiments were generated (Table IV). Among these 20 experiments, six of them were centerpoints, which had the same level of design variables. These centerpoints could be used to check for nonlinearity and reproducibility of the system (27). Hence, no further replications of the design were needed. The experiments were conducted in a randomized order to reduce the effects of any possible factors that were not included in the study, particularly effects that were time dependent. Seven characteristics of the granules produced were determined as the response variables of interest, and they include process yield, mass median diameter (MMD), span, lumps (in percent), fines (in percent), Hausner ratio, and roundness. The possible effects of the design variables on the response variables were examined by fitting the responses to a quadratic model using response surface methodology. Process optimization was then carried out with the following criteria: (a) the percentage of lumps should be minimal and not exceed 2%, *w*/*w*; (b) the Hausner ratio should be within 1–1.2; (c) the span value should be within 1–1.5, and (d) the MMD of the granules should fall within the range of 250–500 μm, with a targeted size of 355 μm.

Part 2

Optimized parameters from part 1 were employed for further study using a Box–Behnken design to understand the effects of inlet airflow rate (X_4), atomizing air pressure (X_5), and distance of spray nozzle to powder bed (X_6). These variables were of interest because they may interact at the side inlet of the product chamber and affect the quality of granules produced. Based on the settings selected (Table IIIb), a total of 18 experiments, including six centerpoints, were generated. The experiments were conducted in a randomized order. Four characteristics of the granules produced were determined as the response variables of interest and they include MMD, span, lumps (in percent), and fines (in percent).

Table IV. Design Variables and Response Variables in the Experiments of Part 1 of this Study

Order		Design variables			Response variables						
StdOrder[a]	RunOrder[a]	X_1	X_2	X_3	Process yield (%)	MMD (μm)	Span	Lumps (%)	Fines (%)	Hausner ratio	Roundness
5	1	350	55	16	92.04	353.0	1.49	4.83	0.88	1.12	2.13
20	2[b]	400	60	14	92.10	414.0	1.38	4.31	0.95	1.11	2.11
11	3	400	50	14	97.05	372.5	1.40	4.22	0.58	1.08	2.19
9	4	300	60	14	88.92	340.5	1.57	3.42	1.07	1.10	2.10
1	5	350	55	12	95.33	347.5	1.54	1.17	2.70	1.08	2.08
8	6	450	65	16	95.66	495.0	1.29	8.01	0.48	1.04	2.19
15	7[b]	400	60	14	93.13	420.0	1.34	3.57	0.99	1.08	2.22
14	8	400	60	18	91.37	422.0	1.35	9.24	0.89	1.11	2.24
17	9[b]	400	60	14	93.56	424.5	1.42	3.37	1.60	1.06	2.27
3	10	350	65	12	94.15	389.0	1.52	1.76	1.12	1.11	2.19
16	11[b]	400	60	14	92.69	407.0	1.31	2.79	0.95	1.06	2.28
10	12	500	60	14	93.55	562.0	1.15	5.08	1.16	1.03	2.23
4	13	450	65	12	94.53	516.0	1.25	1.23	0.81	1.04	2.10
19	14[b]	400	60	14	95.33	436.0	1.38	2.98	1.09	1.05	2.15
2	15	450	55	12	93.16	488.0	1.22	2.61	1.75	1.05	2.33
18	16[b]	400	60	14	93.97	402.5	1.33	3.03	0.43	1.07	2.14
7	17	350	65	16	91.96	391.0	1.48	5.06	2.44	1.10	2.22
13	18	400	60	10	93.39	416.0	1.35	0.15	0.53	1.08	2.20
6	19	450	55	16	92.49	424.0	1.26	6.17	0.60	1.08	2.36
12	20	400	70	14	92.45	455.0	1.43	3.06	1.35	1.08	2.25

[a] StdOrder refers to the original order of the design while RunOrder refers to the exact running order of the experiments after randomization
[b] Denotes centerpoints of the central composite design

Granule Size Analysis

Each granule batch of about 1 kg was first separated into equivalent samples of about 120 g using a spinning riffler (PT, Retsch, Germany). One sample was then sized using a nest of sieves (Endecotts, UK) with descending aperture sizes of 1,400, 1,000, 710, 500, 355, 250, 180, 125, and 90 μm, on a sieve shaker (VS1000, Retsch, Germany) vibrated at 1 mm amplitude for 15 min. The weight of granules retained on each of the sieves was determined and a cumulative undersize distribution plotted. Size parameters, MMD, and span were determined as follows:

$$MMD = D_{50} \tag{2}$$

$$Span = \frac{D_{90} - D_{10}}{D_{50}} \tag{3}$$

where D_{10}, D_{50}, and D_{90} are the particle sizes at 10th, 50th, and 90th percentiles of the cumulative undersize distribution of the particles, respectively. In addition, particles with size less than 90 μm were considered as fines while those with size greater than 1,400 μm were considered as lumps. The fines (in percent) and lumps (in percent) were calculated as follows:

$$Fines = \frac{W_{fines}}{W_{total}} \times 100\% \tag{4}$$

$$Lumps = \frac{W_{lumps}}{W_{total}} \times 100\% \tag{5}$$

where W_{fines}, W_{lumps}, and W_{total} are the weights of the fines, lumps, and the total weight of the particles, respectively.

Flow Properties

Bulk (ρ_b) and tapped (ρ_t) densities of the granules were calculated as the quotients of the weight of the granules in the measuring cylinder and the volume occupied by the granule sample before and after tapping. Tapping (STAV II, JEL Engelsmann, Germany) was carried out according to the USP Method I and the Hausner ratio calculated as follows:

$$Hausner\ ratio = \frac{\rho_t}{\rho_b} \tag{6}$$

Hausner ratio closer to unity indicates better flowability.

Shape Analysis

Granules of size fraction 355–500 μm were gently passed through a 500 μm aperture size sieve. Granules retained on the sieve were then carefully collected for shape analysis using a stereomicroscope (SZH, Olympus, Japan) connected with a video camera (DXC-390, Sony, Japan) and computer. Images collected were analyzed using size analysis software (Image Pro Plus 6.3, Media Cybernetics, USA). A total of 100 granules were examined for each batch. Granule roundness was calculated as follow:

$$Roundness = \frac{P^2}{4\pi A} \tag{7}$$

where P is perimeter and A is area. Roundness is a measure of the circular fit, with a perfect circle having a value of unity.

Drug Content and Content Uniformity

Granules were classified into three fractions: small (size <250 μm); medium (250 ≤ size < 710 μm); and large (size

≥710 μm). About 100 mg of granules were randomly sampled from each size fraction, dissolved in 100 mL of deionized water, and assayed for drug spectrophotometrically (UV-3101 PC, Shimadzu, Japan) at 262 nm. Triplicate analyses were conducted for each class of granules and results averaged.

Statistical Analysis

The statistical analysis and process optimization were carried out using Minitab 16 (Minitab Inc., State College, USA). The quadratic equation used for response surface modeling of the three design variables in Part 1 of this study is shown below.

$$Y = \beta_0 + \beta_1 X_1 + \beta_2 X_2 + \beta_3 X_3 + \beta_{11} X_1^2 + \beta_{22} X_2^2 + \beta_{33} X_3^2 + \beta_{12} X_1 X_2 + \beta_{23} X_2 X_3 + \beta_{13} X_1 X_3 \quad (8)$$

where Y is the response variable; β_0 is a constant; β_1, β_2, and β_3 are the coefficients for the linear terms of X_1, X_2, and X_3, respectively; β_{11}, β_{22}, and β_{33} are the coefficients for the squared terms of X_1^2, X_2^2, and X_3^2 while β_{12}, β_{23}, and β_{13} are the coefficients for the interaction terms of X_1X_2, X_2X_3, and X_1X_3, respectively. Regression analysis was conducted in coded units, where low level was coded as −1 while high level was coded as 1. The level of significance was defined as $p<0.05$. Similar treatment was conducted for X_4, X_5, and X_6 in Part 2 of this study.

Process optimization was conducted by Response Optimizer of Minitab. Once a significant model for each response variable was generated, it formed the design space for the response variable. The desire property of the particular response variable (as above mentioned) could be input for prediction. Therefore, individual desirability value (D value) could be computed. The closer the D value to 1, the closer was the predicted response to the input response. Multiple response variables could be analyzed by the Response Optimizer, taking into the consideration of the target of each response variable. Sets of design variables with different composite D value would then be computed from the individual D values. Similarly, composite D value of closer to 1 was desirable.

RESULTS AND DISCUSSION

This study consisted of two parts. Part 1 was carried out with the aid of DOE to investigate the effects of binder solution and spray distance. It also served to determine the optimal amount of binder solution and other parameters for preparing granules of the desired quality. Part 2 was also carried out with the aid of DOE to investigate the impact of inlet airflow rate, atomizing air pressure, and spray distance on the granulation process. The rationale for splitting the study into two parts was to limit the number of experimental runs required. Consideration of other designs commonly used for DOE studies were reviewed. These included screening designs, such as full factorial design with five factors and three levels, without replications, would result in a total of 243 experiments. On the other hand, Plackett–Burman design with five factors, without replication and centerpoints, required a minimum of 12 experiments. However, Resolution III of Plackett-Burman design meant that the main effects could be confounded by the interaction effects. Furthermore, after screening by Plackett–Burman design, optimization using response surface approaches were still necessary. Therefore, direct use of response surface approach was selected. Nonetheless, a central composite design with five factors required 52 experiments, as suggested by Minitab. Thus, separation of the study to two parts was decided as it reduced the number of experiments. Interaction effects, if any, of X_1, X_2, X_4, and X_5 could not be studied. Nonetheless, as the objective of the second DOE was mainly to further understand the process, the study was carry with the imposed limits in mind. Second, DOE was not involved in the optimization of the process but provided additional information about the process. The above design of studies allowed the estimation of the working ranges for important basic variables, such as amount and spray rate of binder solution which is crucial for investigation of other parameters.

First DOE by Central Composite Design

Results of the first DOE are shown in Table IV using ANOVA and response surface modeling, the results were analyzed to determine possible main effects and interaction effects of the variables (Table V). All the response variables showed insignificant lack of fit ($p>0.05$) to the quadratic equation However, only MMD, span, percentage of lumps, and Hausner ratio showed statistically significant models while the rest of the response variables did not. Therefore, the equations that showed the effects of the design variables on each of these response variables were derived. The descriptive statistics of the centerpoints are shown in Table VI. Low coefficients of variation (<10%) were found for process yield, MMD, span, Hausner ratio, and roundness. These findings were indicative that the FlexStream™ fluidized bed granulation was able to reproduce consistent end products.

Influence of Design Variables of First DOE on Process Yield

During the granulation process, fine feed powder was subjected to a swirling air flow from the bottom of the product chamber. Some fines might be blown to the sock filters due to relatively high initial air flow rate. Nonetheless, throughout the granulation process, blow back air jets at the sock filters helped to dislodge the fines and return them back into the product chamber for granulation. As shown in Table V, all the design variables had no significant effect on the process yield. No significant model could be developed to describe the relationship between process yield and the granulation process ($p=0.143$). However, high process yields that ranged from 88.92% to 97.05% were possible within the range of parameters studied (Table IV). This indicated that FlexStream™ fluidized bed granulation had high process yields with relative insensitivity to the amount of binder solution delivered, spray rate of binder solution and distance between spray nozzle and powder bed.

Influence of Design Variables of First DOE on Granule Size and Size Distribution

The MMD of the granules ranged from 340.5 to 562.0 μm (Table IV). Table V shows that a significant model ($p=0.000$) was successfully developed to describe the relationship

Table V. Results of ANOVA and Response Surface Modeling for Part 1 of the Study

Coefficient	Process yield	MMD	Span	Lumps	Fines	Hausner ratio	Roundness
β_0	93.591[a]	417.352[a]	1.361[a]	3.319[a]	1.074[b]	1.072[a]	2.196[a]
β_1	0.727	55.344[a]	−0.115[a]	0.532[b]	−0.207	−0.021[b]	0.039[c]
β_2	−0.370	21.469[a]	0.006	−0.065	0.030	−0.002	−0.005
β_3	−0.566	−4.094	−0.001	2.218[a]	−0.078	0.006	0.018
β_{11}	−0.492	8.489[b]	0.001	0.216	0.064	−0.002	−0.007
β_{22}	0.387	−0.886	0.015[c]	0.062	0.027	0.001	0.006
β_{33}	−0.206	0.426	−0.001	0.327[c]	−0.037	0.006	0.006
β_{12}	0.726	2.438	0.012	−0.045	−0.131	−0.006	−0.075[b]
β_{13}	0.742	−11.562[c]	0.023	0.420	−0.122	0.001	0.004
β_{23}	0.361	4.937	0.003	0.356	0.496[c]	−0.010	0.005
R^2 (%)	64.58	97.52	95.50	95.43	45.75	78.08	70.34
$R^2_{predicted}$ (%)	0.00	88.27	86.27	75.68	0.00	54.32	8.53
$R^2_{adjusted}$ (%)	32.70	95.28	91.44	91.32	0.00	58.36	43.64
Regression	0.143	0.000[d]	0.000[d]	0.000[d]	0.534	0.021[d]	0.074
Linear	0.122	0.000[d]	0.000[d]	0.000[d]	0.574	0.003[d]	0.084
Square	0.164	0.032[d]	0.205	0.113	0.920	0.321	0.752
Interaction	0.271	0.090	0.233	0.192	0.185	0.312	0.030
Lack of fit significance	0.182	0.479	0.888	0.271	0.062	0.984	0.879

[a] 0.001 level, statistical significance
[b] 0.01 level, statistical significance
[c] 0.05 level, statistical significance
[d] Denotes statistically significant model

between the design variables and MMD, and there was insignificant lack of fit of the model (p=0.479). The linear (p=0.000) and square (p=0.032) effects were found to be significant. Theoretically, R^2 describes the variation in responses that are explained by the model whereas $R^2_{predicted}$ reflects how well the model could predict future data. $R^2_{predicted}$ is calculated from prediction sum of square (PRESS) value of the model derived from cross validation by Minitab. For each potential model, Minitab omits one observation and recalculates the model. Following this, the recalculated model will be used to predict the omitted observation to generate cross-validated fitted value. Cross-validated residual value is then calculated by comparing the cross-validated fitted value and the omitted observation. This process is repeated until all observations have been omitted and fitted. Next, PRESS and $R^2_{predicted}$ could be calculated. As R^2 always increase as terms are added to the model, $R^2_{adjusted}$ is a more useful indicator of the variation in responses (28). Based on the $R^2_{adjusted}$ (95.28%) and $R^2_{predicted}$ (88.27%) values obtained, it could be inferred that the model developed could explain the variations well and good in prediction. ANOVA showed that MMD was significantly affected by the amount of binder solution delivered and binder solution spray rate (Table V). The squared term of amount of binder solution delivered was also found to be significant in affecting MMD of the granules, indicating that the amount of binder solution had a greater effect than the other variables on the MMD and it was not a linear effect. These observations were in agreement with the findings of the other reported studies (14,15), where such observations were associated with the formation of mobile liquid bonds responsible for increased cohesiveness of the mass (29). Contour plot of the results showed steady rise in MMD with increase in the amount of binder solution used (Fig. 2a). This trend was also observed for the binder solution spray rate. Other workers had reported that an increased binder solution spray rate resulted in increased spray droplet size and moisture content in the product chamber which favored granule growth (7,16,17,30,31). ANOVA (Table V) also showed that the interaction of amount of binder solution delivered and distance between spray nozzle and powder bed had a significant negative contribution to MMD. As further illustrated by the contour plot, the effect of amount of binder solution delivered decreased with increasing distance between spray nozzle and powder bed (Fig. 2b). This finding was in agreement with those previously reported (16,32).

Table VI. Descriptive Statistics of the six Centerpoints in the Central Composite Design

Response variables	Mean	Standard deviation	Coefficient of variation (%)
Process yield (%)	93.46	1.12	1.20
MMD (μm)	417.3	12.21	2.93
Span	1.36	0.04	2.94
Lumps (%)	3.34	0.55	16.50
Fines (%)	1.00	0.37	37.00
Hausner ratio	1.07	0.02	1.87
Roundness	2.20	0.07	3.18

The percentages of lumps in these experiments were found to range from 0.15% to 9.24% (Table IV). Table V shows that a significant model (p=0.000) was available to describe the effects of design variables on percentage of lumps in the granule batches. This model had relatively high $R^2_{adjusted}$ (91.32%) and $R^2_{predicted}$ (75.68%) values. ANOVA revealed that the amount of binder solution and distance between spray nozzle and powder bed had significant effects on the percentage of lumps produced (Table V). It could be seen from the contour plot that spray nozzle located further away from powder bed resulted in more lumps, possibly due to the weaker shearing action by atomizing air pressure (Fig. 2c). Significant squared term indicated a nonlinear relationship between distance between spray nozzle and powder bed and percentage of lumps.

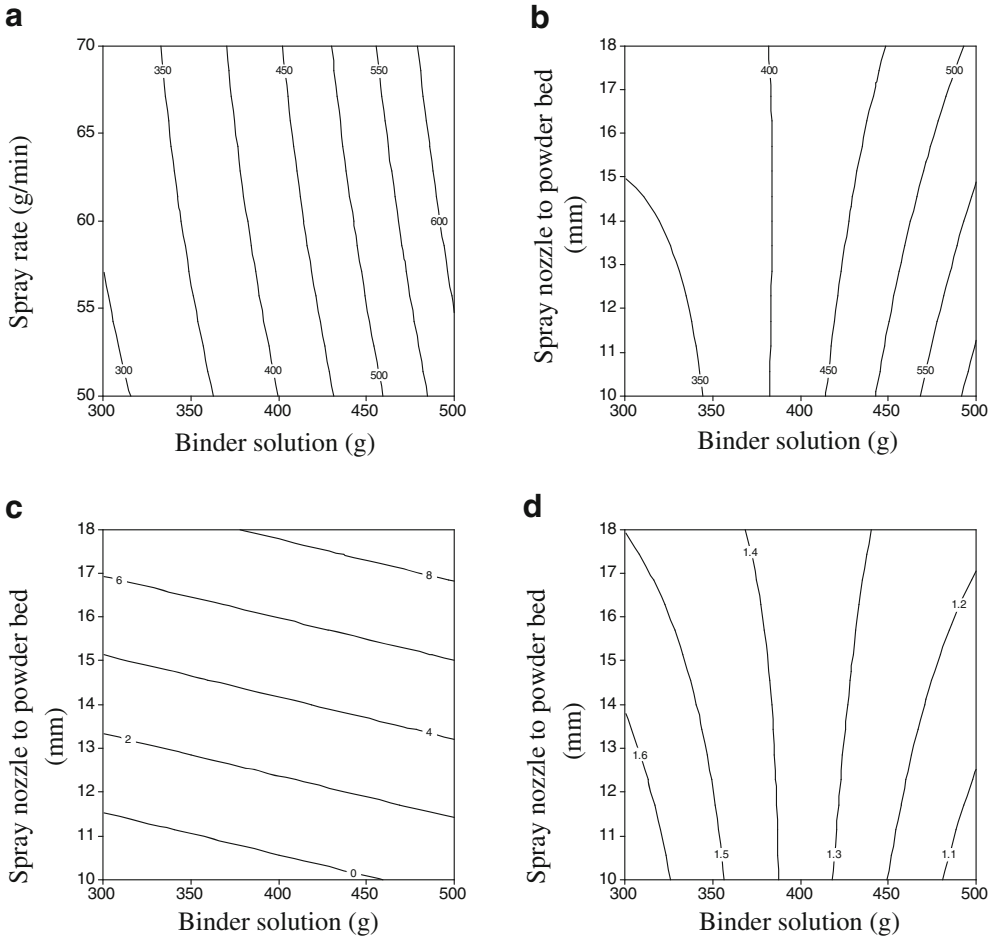

Fig. 2. Contour plots of the effect of **a** amount of binder solution delivered and binder solution spray rate (hold value at distance between spray nozzle and powder bed=10 mm) on MMD; **b** amount of binder solution delivered and distance between spray nozzle and powder bed (hold value at binder solution spray rate=60 g/min) on MMD; **c** amount of binder solution delivered and distance between spray nozzle and powder bed(hold value at binder solution spray rate=60 g/min) on lump (in percent); **d** amount of binder solution delivered and distance between spray nozzle and powder bed (hold value at binder solution spray rate=60 g/min) on span

Figure 2c also shows that the amount lumps increased with the amount of binder solution delivered, which was expected.

Span of the granules produced ranged from 1.15 to 1.57. Table V shows that a significant fitting model (p= 0.000) was developed for span, with high R^2_{adjusted} (91.44%) and $R^2_{\text{predicted}}$ (86.27%) values. ANOVA indicated that the amount of binder solution had linear effect on span of the granules produced (Table V). A negative coefficient suggested that the amount of binder solution delivered contributed negatively to span (Fig. 2d), as also reported by other investigators (6,14). In addition, squared binder solution spray rate showed a small positive effect on span (Table V). This was due possibly to the wider size distribution of the droplets (33), resulting in granules with wider size distribution.

Fines in these experiments ranged from 0.43% to 2.70%. No statistically significant model could be developed to correlate fines with the design variables (Table V). ANOVA showed that only interactive effect between binder solution spray rate and distance between spray nozzle and powder bed had significant effect on the amount of fines produced (Table V). This observation meant that an increase in distance between spray nozzle and powder bed had resulted in increased amount of fines for a particular binder solution spray rate. A decrease of binder droplet number with distance traveled had contributed to this observation.

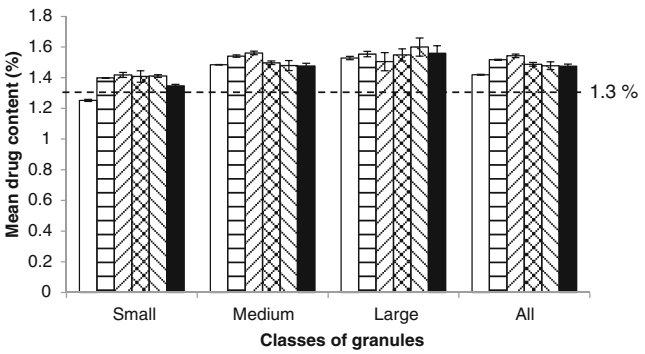

Fig. 3. Mean drug content for small, medium, large and overall granule batch of batch 2 (□), batch 7 (▤), batch 9 (▨), batch 11 (▩), batch 14 (▧), and batch 16 (■) in central composite design. *Dotted line* the theoretical drug content

Table VII. Optimized Conditions for FlexStream™ Fluidized Bed Granulation Process

	Optimized parameters with highest D-value			Optimized parameters chosen for use		
	Binder solution (g)	Spray rate (g/min)	Spray nozzle to powder (mm)	Binder solution (g)	Spray rate (g/min)	Spray nozzle to powder (mm)
	435.4	50.00	10.08	415	60.00	10
Lumps (%)		−0.04			−0.47	
Hausner ratio		1.04			1.08	
Span		1.29			1.31	
MMD (μm)		455.8			451.5	
Composite desirability (*D* value)		0.70			0.64	

Influence of Design Variables of First DOE on Hausner Ratio

Hausner ratio of the granules produced ranged from 1.03 to 1.12 (Table IV). A statistically significant fitting model (p= 0.021) describing the relationship of Hausner ratio with the design variables was established (Table V). However, the $R^2_{adjusted}$ (58.36%) and $R^2_{predicted}$ (54.32%) values (Table V) showed that this model did not fit as well as the other previous models discussed. Flow properties of materials are known to be affected by several factors, such as bulk density, size, shape, surface roughness, moisture content, and cohesiveness of the materials. The relatively low $R^2_{adjusted}$ and lower $R^2_{predicted}$ values could be attributed to the exclusion of these factors. Nonetheless, ANOVA showed that the amount of binder solution had a significant effect on Hausner ratio (Table V). MMD was previously found to increase with the amount of binder solution delivered. This increase in particle size with amount of binder solution delivered aptly accounted for the better flowability of the granules produced (34,35).

Influence of Design Variables of First DOE on Shape of Granules

Roundness of the granules ranged from 2.08 to 2.36 (Table IV). No statistically significant model was developed for roundness of the granules but amount of binder solution delivered and interaction effect of amount of binder solution delivered and binder solution spray rate were found to be statistically significant in affecting roundness of the granules (Table V). Concurrent increase in amount and spray rate of binder solution would intensify the binder action, as well as moisture content in the processor. This would in turn imparted higher plasticity and deformability to the granules (36) and rendered them with better deformability. Coupled with the higher degree friction conferred by the in swirling air flow (37) in the product chamber, the moistened granules were kneaded against the wall and each other, producing rounder granules.

Drug Content and Content Uniformity

Process parameters for the six centerpoints in the DOE were similar. Therefore, granules made under these conditions were selected for investigation of drug content and content uniformity of the granules produced. Figure 3 shows that drug content increased from small to large granules. This was expected as larger granules received more binder solution that contained the drug. Nonetheless, the overall drug content in the batch of was found to be close to the theoretical drug content estimated by calculation (1.3%). Narrow standard deviation observed (Fig. 3) suggested very uniform drug distribution.

Optimization of Granulation Process

Table VII shows the optimized parameters derived from the results with the aid of Minitab 16. Composite *D* value is a measure of the accuracy of prediction. The closer the response to the target, the closer the *D* value is to one. Therefore, the optimized parameters with *D* values of 0.70 were considered to be fairly accurate in producing granules with the desired characteristics. However, these optimized parameters were not the best operating parameters from the technical point of view. It was operationally challenging to deliver the binder solution at a distance of 10.08 mm between the spray nozzle and powder bed. Furthermore, a higher binder solution spray rate would be preferable to shorten the processing time. Taking the above into consideration, the optimized parameters with a slightly lower composite *D* value of 0.64 were chosen, as shown in Table VII. As the composite *D* value was generated by analyzing the significant models simultaneously, by changing the other two design variables, *i.e.*, spray rate and distance of spray nozzle to powder bed, a slightly lower amount of binder solution (415 g) was predicted to be sufficient to produced granules that close to the target set.

Table VIII. Predicted and Actual Characteristics of Granules Prepared Under Optimized Conditions

	Actual characteristic					
	1	2	3	Mean (SD)	Predicted characteristic	Difference actual *vs.* predicted (%)
Lumps (%)	0.16	0.15	0.14	0.15 (0.01)	−0.47	N.A.
Hausner ratio	1.17	1.15	1.15	1.16 (0.01)	1.08	6.90
Span	1.30	1.28	1.30	1.29 (0.01)	1.31	1.55
MMD (μm)	399.5	405.0	404.0	402.8 (2.93)	451.5	12.09

Table IX. Design Variables and Response Variables in the Experiments of Part 2 of this Study

Order		Design variables			Response variables			
StdOrder[a]	RunOrder[a]	X_4	X_5	X_6	MMD (μm)	Span	Lumps (%)	Fines (%)
16	1[b]	100	2.5	14	343.5	1.52	5.46	3.74
7	2	80	2.5	18	351.0	1.44	9.99	0.91
15	3[b]	100	2.5	14	353.5	1.46	2.53	3.70
9	4	100	1.5	10	440.0	1.42	0.14	3.32
8	5	120	2.5	18	296.0	1.81	3.93	11.70
4	6	120	3.5	14	268.0	1.82	1.59	11.02
2	7	120	1.5	14	369.0	1.60	2.83	9.93
6	8	120	2.5	10	299.5	1.70	0.13	9.69
5	9	80	2.5	10	398.5	1.36	1.81	0.61
18	10[b]	100	2.5	14	351.5	1.46	4.02	3.21
11	11	100	1.5	18	415.5	1.35	12.37	2.61
12	12	100	3.5	18	307.5	1.67	7.71	4.84
17	13[b]	100	2.5	14	341.5	1.52	4.52	4.17
13	14[b]	100	2.5	14	350.5	1.41	5.79	0.74
14	15[b]	100	2.5	14	333.5	1.53	5.08	3.71
10	16	100	3.5	10	287.5	1.63	0.46	6.29
1	17	80	1.5	14	465.5	1.43	7.58	4.53
3	18	80	3.5	14	313.0	1.65	3.40	5.56

[a] StdOrder refers to the original order of the design while RunOrder refers to the exact running order of the experiments after randomization
[b] Denotes centerpoints of the Box–Behnken design

Replicated granulation runs were conducted according to the chosen optimized parameters. The characteristics of the granules produced were examined and compared with predicted values (Table VIII). According to the model developed, the amount of fines would be −0.47%, which is negligible and comparable to the actual value of 0.15%. Furthermore, the difference between the actual and predicted characteristics was about 12% and less. Moreover, the granules produced exhibited the desirable characteristics specified. Hence, the optimized runs were deemed as successful and within expectation.

Table X. Results of ANOVA and Response Surface Modeling for Part 2 of the Study

Coefficient	MMD	Span	Lumps	Fines
β_0	345.667[a]	1.484[a]	4.566[a]	3.212[b]
β_1	−36.938[a]	0.132[b]	−1.787[b]	3.842[b]
β_2	−64.250[a]	0.120[b]	−1.219[c]	0.914
β_3	−6.938	0.019	3.933[a]	0.019
β_{11}	−9.083	0.101[c]	−0.960	3.005[b]
β_{22}	17.292[b]	0.040	0.244	1.544
β_{33}	−0.333	−0.006	0.358	−0.492
β_{12}	12.875[c]	−0.000	0.735	0.017
β_{13}	11.000[c]	0.008	−1.096	0.426
β_{23}	11.125[c]	0.028	−1.245	−0.186
R^2 (%)	98.78	89.74	92.58	89.26
$R^2_{\text{predicted}}$ (%)	89.29	0.00	34.00	0.00
R^2_{adjusted} (%)	97.42	78.21	84.24	77.18
Regression	0.000[d]	0.004[d]	0.001[d]	0.005[d]
Linear	0.000[d]	0.001[d]	0.000[d]	0.001[d]
Square	0.012[d]	0.051	0.511	0.014[d]
Interaction	0.010[d]	0.862	0.138	0.954
Lack of fit significance	0.280	0.132	0.272	0.137

[a] 0.001 level, statistical significance
[b] 0.01 level, statistical significance
[c] 0.05 level, statistical significance
[d] Denotes statistically significant model

Second DOE by Box–Behnken Design

With the optimized parameters, the second DOE was carried out to investigate the effects of inlet airflow rate (X_4), atomizing air pressure (X_5), and distance between spray nozzle and powder bed (X_6). In the first DOE, the effects of the operating parameters mainly affected the MMD, span, lumps (in percent), and fines (in percent) of the product. Hence, these properties constituted the response variables in the second DOE. Design settings and the response variables of all the experiments are shown in Table IX.

Influence of Design Variables of Second DOE on Granule Size and Granule Size Distribution

Physical characteristics of the granules produced are shown in Table IX. Statistically significant models were developed for describing the relationship between the design variables (X_4, X_5, and X_6) and response variables (Table X). ANOVA showed that inlet airflow rate and atomizing air pressure had significant effects on MMD, span, and percentage of lumps. Both inlet airflow rate and atomizing air pressure had negative effects on MMD and percentage of lumps. Increased rate of evaporation was expected with increasing air flow rate due to improved heat transfer coefficient (30,38). Therefore, the potential for good wetting and agglomeration of the particles would be impaired. Furthermore, powder bed would expand with increased inlet airflow rate, thereby increasing interparticle distances. Under these production conditions, the particles had possessed high kinetic energies would show increased in attritive tendencies (38). The negative effect of atomizing air pressure was in agreement with previously reported results (16,17,39). Schœfer *et al.* had shown that granule size was directly proportional to droplet size. As atomizing air pressure increased, smaller binder droplets were produced (33), resulting in smaller granules. Effects

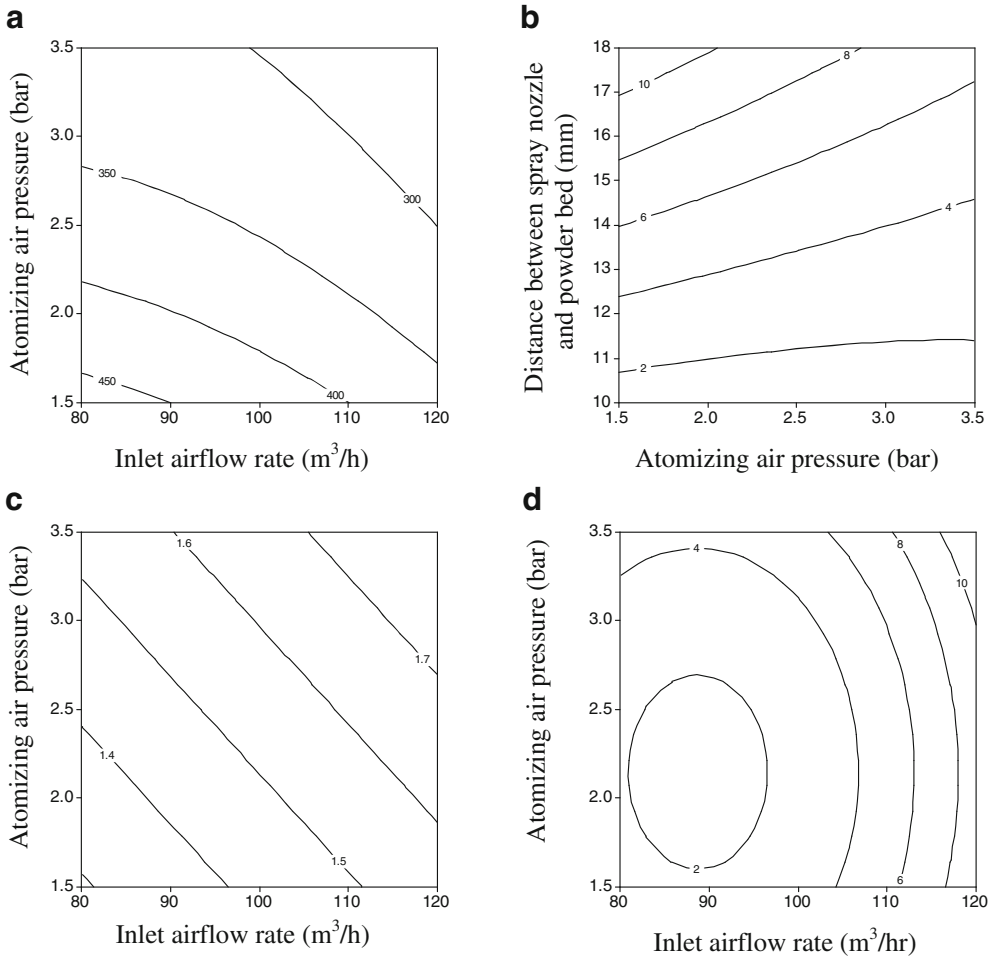

Fig. 4. Contour plots of the effect of **a** inlet airflow rate and atomizing air pressure (hold value at distance between spray nozzle and powder bed=14 mm) on MMD; **b** atomizing air pressure and distance between spray nozzle and powder bed (hold value at inlet airflow rate=100 m^3/h) on lumps (in percent); **c** inlet airflow rate and atomizing air pressure (hold value at distance between spray nozzle and powder bed=14 mm) on span; **d** inlet airflow rate and atomizing air pressure (hold value at distance between spray nozzle and powder bed=10 mm) on fines (in percent)

of inlet airflow and atomizing air pressure on MMD are depicted in Fig. 4a. In addition, distance between spray nozzle and powder bed was found to have significant positive effect on percentage of lumps (Table X), which agreed with the findings of the first DOE. Figure 4b depicts this relationship. In contrast, inlet airflow rate and atomizing air pressure had significant positive effect on span (Fig. 4c), as these conditions did not favor agglomeration. Nonetheless, only inlet airflow rate was found to have significant positive effect on the percentage of lumps (Table X). Increase in airflow rate impeded the agglomeration of the fine particles, leading to increased percentage of fines (Fig. 4d).

Squared term of atomizing air pressure (Table X) was found to be statistically significant, indicating that atomizing air pressure and MMD followed nonlinear relationship. Similarly, inlet airflow rate and span or percentage of fines also followed nonlinear relationships.

CONCLUSION

The operational and capability of the FlexStream™ fluidized bed processor with swirling airflow were successfully investigated using two DOE studies. It was established that the amount of binder solution affected the size, size distribution, flowability, and roundness of the granules, as well as the percentage of lumps produced. The amount of binder solution had a positive correlation with granule size and percentage of lumps but a negative correlation with size distribution and Hausner ratio. Binder solution spray rate also affected granule size positively while the distance between spray nozzle and powder bed exerted similar effect on the percentage of lumps. Some of the interaction effects were statistically significant in affecting the characteristics of the granules. In addition, overall drug content uniformity of granules was found to be high.

Models were successfully developed to describe the relationships between specific variables and responses. Optimized parameters were derived and employed to investigate other factors. It was shown that inlet airflow rate and atomizing air pressure had a negative effect on granule size and percentage of lumps but a positive effect on size distribution. The percentage of fines was significantly affected by inlet airflow rate. The distance between spray nozzle and powder bed showed a positive effect on the percentage of lumps produced.

ACKNOWLEDGMENTS

The authors would like to acknowledge the financial support from GEA-NUS PPRL fund (N-148-000-008-001) and A*STAR SERC grant no. 102 161 0049 (R-148-000-157-305). Wong Poh Mun is a recipient of the National University of Singapore Graduate Research Scholarship.

REFERENCES

1. Schœfer T, Worts O. Control of fluidized bed granulation I. Effects of spray angle, nozzle height and starting materials on granule size and size distribution. Arch Pharm Chem Sci. 1977;5:51–60.
2. Schœfer T, Worts O. Control of fluidized bed granulation II. Estimation of droplet size of atomized binder solutions. Arch Pharm Chem Sci. 1977;5:178–93.
3. Schœfer T, Worts O. Control of fluidized bed granulation III. Effects of inlet air temperature and liquid flow rate on granule size and size distribution. Control of moisture content of granules in the drying phase. Arch Pharm Chem Sci. 1978;6:1–13.
4. Schœfer T, Worts O. Control of fluidized bed granulation IV. Effects of binder solution and atomization on granule size and size distribution. Arch Pharm Chem Sci. 1978;6:14–25.
5. Schœfer T, Worts O. Control of fluidized bed granulation V. Factors affecting granule growth. Arch Pharm Chem Sci. 1978;6:69–82.
6. Alkan MH, Yuksel A. Granulation in a fluidized bed. II. Effect of binder amount on the final granules. Drug Dev Ind Pharm. 1986;12(10):1529–43.
7. Kokubo H, Sunada H. Effect of process variables on the properties and binder distribution of granules prepared in a fluidized bed. Chem Pharm Bull. 1997;45(6):1069–72.
8. Schaafsma SH, Vonk P, Kossen NWF. Fluid bed agglomeration with a narrow droplet size distribution. Int J Pharm. 2000;193 (2):175–87.
9. Rajniak P, Mancinelli C, Chern RT, Stepanek F, Farber L, Hill BT. Experimental study of wet granulation in fluidized bed: impact of the binder properties on the granule morphology. Int J Pharm. 2007;334(1–2):92–102.
10. Nienow AW, Rowe PN. Particle growth and coating in gas-fluidized beds. In: Davidson JF, Clift R, Harrison D, editors. Fluidization. 2nd ed. Orlando: Academic; 1985. p. 563–94.
11. Yilmaz M, Çomakli O, Yapici S. Enhancement of heat transfer by turbulent decaying swirl flow. Energy Convers Manag. 1999;40 (13):1365–76.
12. Algifri AH, Bhardwaj RK, Rao YVN. Heat transfer in turbulent decaying swirl flow in a circular pipe. Int J Heat Mass Transf. 1988;31(8):1563–8.
13. Özbey M, Söylemez MS. Effect of swirling flow on fluidized bed drying of wheat grains. Energy Convers Manag. 2005;46(9–10):1495–512.
14. Ritala M, Virtanen S. The effect of binder solution quantity and lactose particle size on granule properties. Acta Pharma Nordica. 1991;3(4):229–34.
15. Niskanen T, Niskanen M, Yliruusi J, Kristoffersson E. Granulation in instrumented fluidized bed granulator—evaluation of the effects of two independent process variables on granule properties. Acta Pharma Nordica. 1991;3(1):19–24.
16. Davies WL, Gloor Jr WT. Batch production of pharmaceutical granulations in a fluidized bed. I. Effects of process variables on physical properties of final granulation. J Pharm Sci. 1971;60(12):1869–74.
17. Rambali B, Baert L, Thone D, Massart DL. Using experimental design to optimize the process parameters in fluidized bed granulation. Drug Dev Ind Pharm. 2001;27(1):47–55.
18. Arnaud P, Brossard D, Chaumeil JC. Effect of the granulation process on nitrofurantoin granule characteristics. Drug Dev Ind Pharm. 1998;24(1):57–66.
19. Hausman DS. Comparison of low shear, high shear, and fluid bed granulation during low dose tablet process development. Drug Dev Ind Pharm. 2004;30(3):259–66.
20. Aulton ME. Drying. In: Aulton ME, editor. Aulton's pharmaceutics: the design and manufacture of medicines. 3rd ed. New York: Churchill Livingstone; 2007. p. 425–40.
21. Er DZL, Liew CV, Heng PWS. Layered growth with bottom-spray granulation for spray deposition of drug. Int J Pharm. 2009;377(1–2):16–24.
22. Loh ZH, Er DZ, Chan LW, Liew CV, Heng PW. Spray granulation for drug formulation. Expert Opin Drug Deliv. 2011;8 (12):1645–61.
23. Liew CV, Er DZL, Heng PWS. Air-dictated bottom spray process: Impact of fluid dynamics on granule growth and morphology. Drug Dev Ind Pharm. 2009;35(7):866–76.
24. Schaafsma SH, Kossen NWF, Mos MT, Blauw L, Hoffmann AC. Effects and control of humidity and particle mixing in fluid-bed granulation. AICHE J. 1999;45(6):1202–10.
25. Jager, Bauer. Effects of material motion on agglomeration in the rotary fluidized bed granulator. Drugs Made Ger. 1982;25:61–5.
26. Kristensen J, Hansen VW. Wet granulation in rotary processor and fluid bed: comparison of granule and tablet properties. AAPS PharmSciTech. 2006;7(1):E1–10.
27. Esbensen KH, Guyot D, Westad F, Houmøller LP. 16. Introduction to experimental design. Multivariate data analysis —in practice: an introduction to multivariate data analysis and experimental design. 5th ed: Camo Software; 2001.
28. Myers RH, Montgomery DC. Building empirical model. Response surface methodology: process and product optimization using designed experiments. 2nd ed. New York: Wiley; 2002. p. 17.
29. Kristensen HG, Holm P, Jaegerskou A, Schaefer T. Granulation in high-speed mixers. 4. Effect of liquid saturation on the agglomeration. Pharm Ind. 1984;46(7):763–7.
30. Hemati M, Cherif R, Saleh K, Pont V. Fluidized bed coating and granulation: influence of process-related variables and physicochemical properties on the growth kinetics. Powder Technol. 2003;130(1–3):18–34.
31. Lipps DM, Sakr AM. Characterization of wet granulation process parameters using response surface methodology. 1. Top-spray fluidized bed. J Pharm Sci. 1994;83(7):937–47.
32. Rankell AS, Scott MW, Lieberman HA, Chow FS, Battista JV. Continuous production of tablet granulations in a fluidized bed. II. J Pharm Sci. 1964;53:320–4.
33. Wan LSC, Heng PWS, Liew CV. The influence of liquid spray rate and atomizing pressure on the size of spray droplets and spheroids. Int J Pharm. 1995;118(2):213–9.
34. Pilpel N. The flow properties of magnesia. J Pharm Pharmacol. 1964;16:705–16.
35. Jones TM, Pilpel N. The flow properties of granular magnesia. J Pharm Pharmacol. 1966;18(2):81–93.
36. Andersson KM, Bergström L. Friction and adhesion of single spray-dried granules containing a hygroscopic polymeric binder. Powder Technol. 2005;155(2):101–7.
37. Yilmaz M, Comakli O, Yapici S, Sara ON. Heat transfer and friction characteristics in decaying swirl flow generated by different radial guide vane swirl generators. Energy Convers Manag. 2003;44(2):283–300.
38. Scott MW, Lieberman HA, Rankell AS, Battista JV. Continuous production of tablet granulations in a fluidized bed. I. J Pharm Sci. 1964;53:314–20.
39. Lin K, Peck GE. Development of agglomerated talc. I. Evaluation of fluidized bed granulation parameters on the physical properties of agglomerated talc. Drug Dev Ind Pharm. 1995;21(4):447–60.